

Sintering-resistant Pt@CeO₂ nanoparticles for high-temperature oxidation catalysis

Siwon Lee^a, Jongsu Seo^a, and WooChul Jung^{a,*}

^a*Department of Materials Science and Engineering, Korea Advanced Institute of Science and Technology (KAIST), 291 Daehak-ro, Yuseong-gu, Daejeon, 305–701, Republic of Korea*

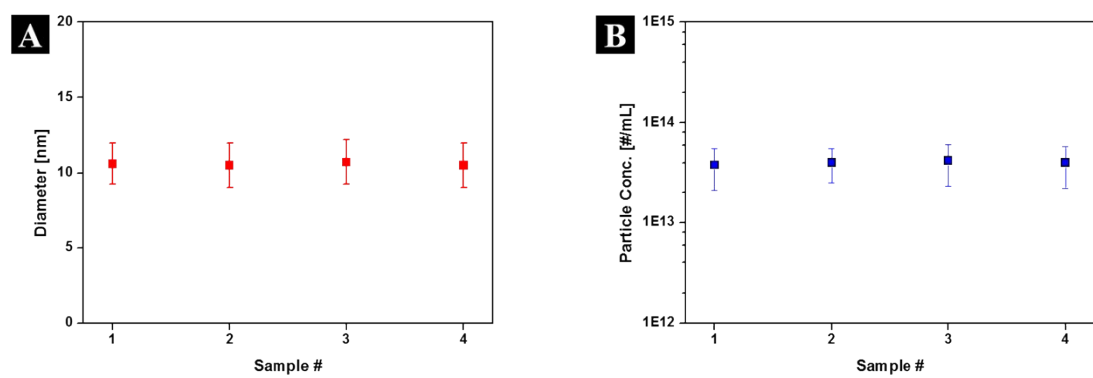


Fig. S1. The graphs of (A) an average diameter, and (B) an average particle concentration of each Pt nanoparticle, synthesized under the same condition.

Table S1. Results of reproducibility on synthesized Pt nanoparticles.

^a Sample #	sample 1	sample 2	Sample 3	sample 4
^b Average diameter [nm]	10.6 ± 1.4	10.5 ± 1.5	10.7 ± 1.5	10.5 ± 1.5
ICP-MS [ppm]	493.3	476.8	527.2	499.3
^c Particle Concentration [# mL ⁻¹]	3.8 (± 1.7) × 10 ¹³	4.0 (± 1.5) × 10 ¹³	4.2 (± 1.9) × 10 ¹³	4.0 (± 1.8) × 10 ¹³

^aSample 1-4 (Pt nanoparticles) were synthesized under the same condition at different days.

^bAverage diameter of each sample was evaluated by counting 200 different particles.

^c Particle concentration was calculated by assuming sphere-shaped particles and using average diameters, a density of Pt (21.46 g cm⁻³) and ICPMS results.

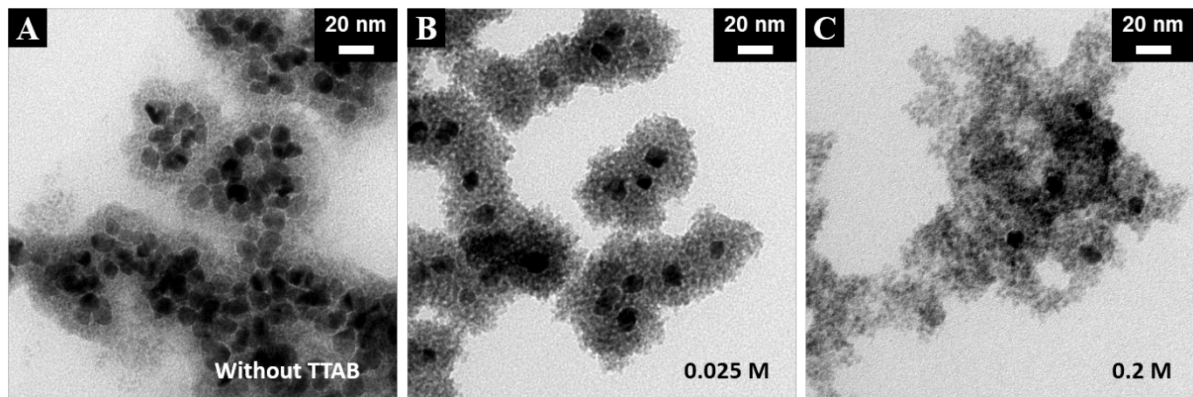


Fig. S2. TEM images of Pt@CeO₂ nanocomposites synthesized with different amount of TTAB surfactant. (A) without TTAB, (B) 0.025 M of TTAB, and (C) 0.2 M of TTAB. Individual Pt nanoparticles are distantly encapsulated by ceria shells with a uniform shell thickness when the concentration of TTAB is optimized at 0.025M.

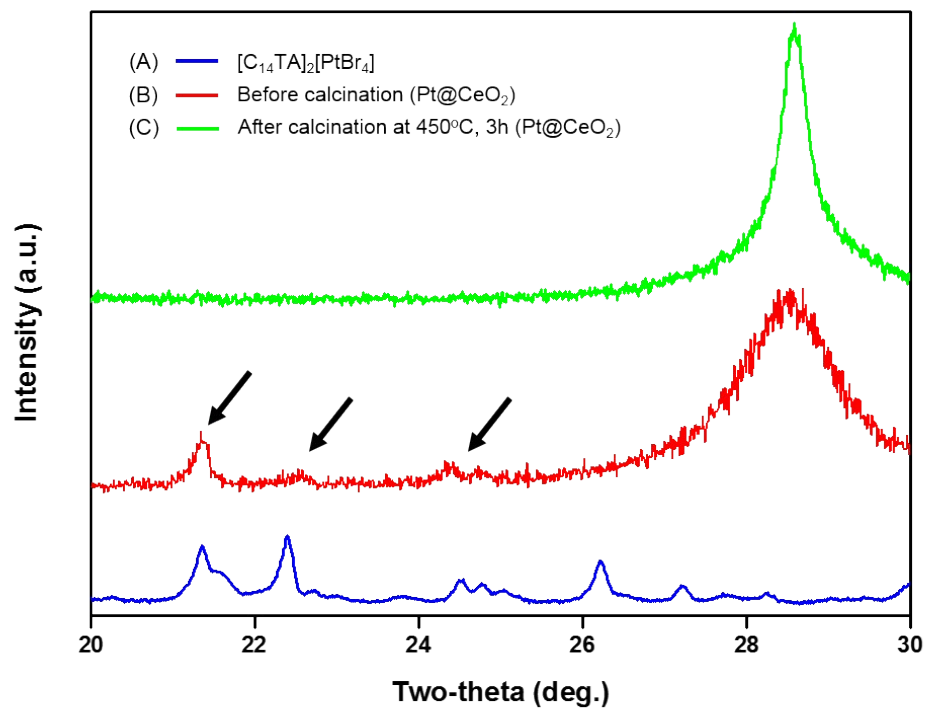


Fig. S3. The XRD pattern of $[\text{C}_{14}\text{TA}]_2[\text{PtBr}_4]$ (A). The XRD pattern of $\text{Pt}@\text{CeO}_2$ nanocomposite before (B) and after (C) calcination at 450°C for 3 hours.

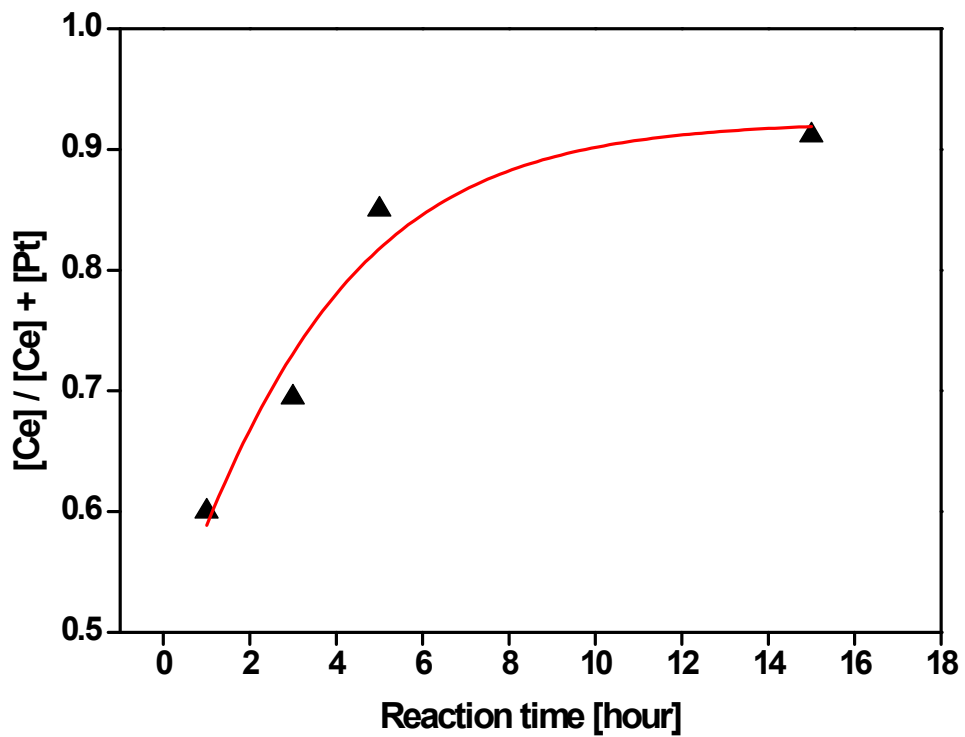


Fig. S4. The concentration of Pt@CeO₂ nanocomposite with respect to the reaction time, showing that continuous heterogeneous nucleation occurs until all of the cerium precursors are consumed.

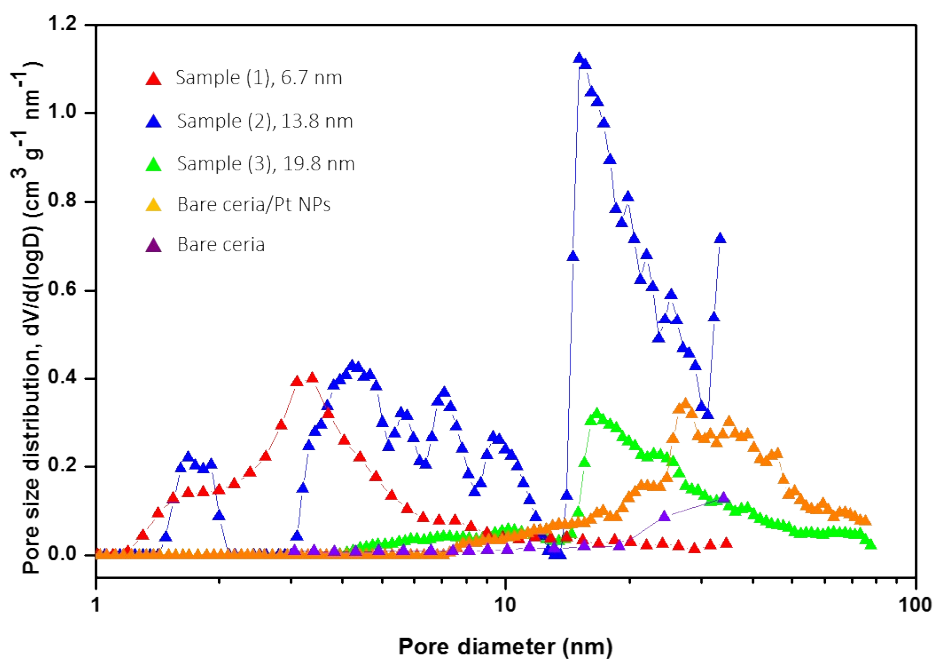


Fig. S5. Pore size distributions for five different samples. Pt@CeO₂ core-shell composites with the shell thickness of 6.7 nm (red triangle), 13.8 nm (blue triangle) and 19.8 nm (green triangle), a bare mixture of Pt and ceria (orange triangle) and a pure ceria (purple triangle).

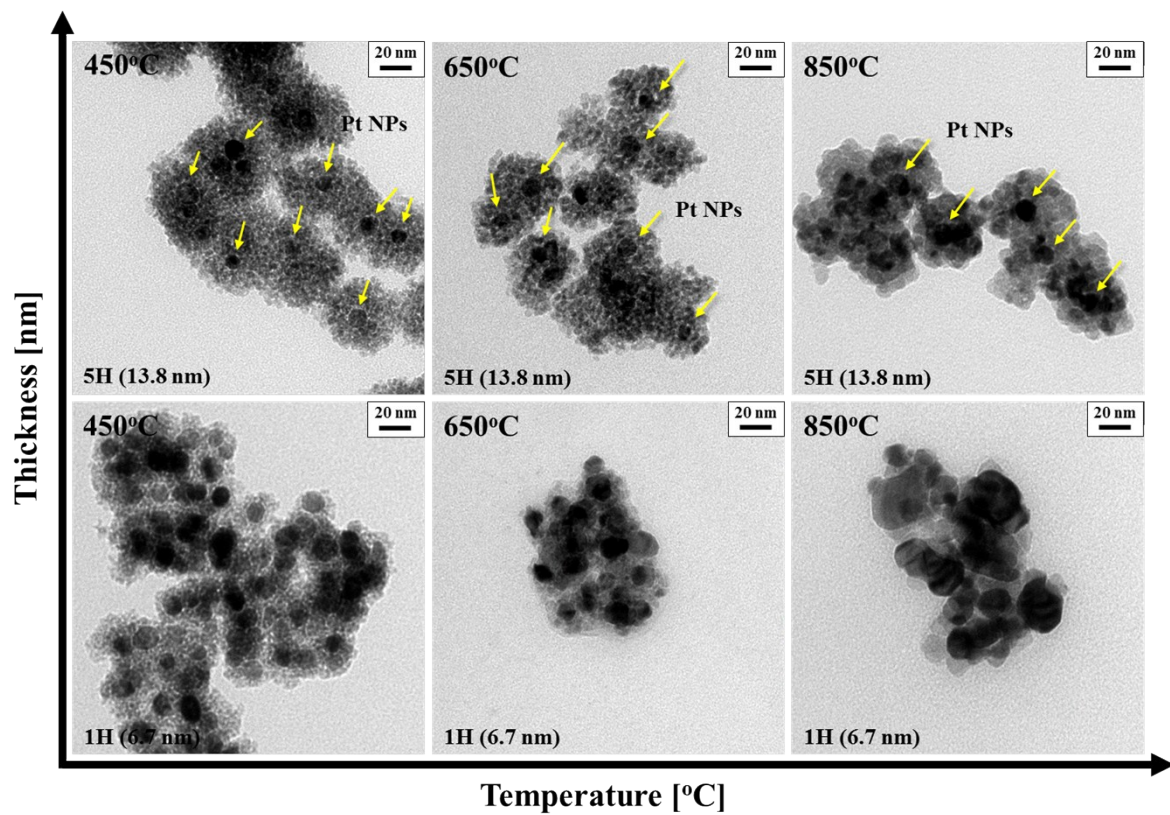


Fig. S6. TEM images showing the morphological change of Pt@CeO₂ nanocomposites upon annealing for two different samples (Pt@CeO₂ (6.7 nm) – first row, Pt@CeO₂ (13.8 nm) – second row). All the samples were calcined at 450 °C to remove any remaining organic materials. (450 °C: as-synthesized sample)

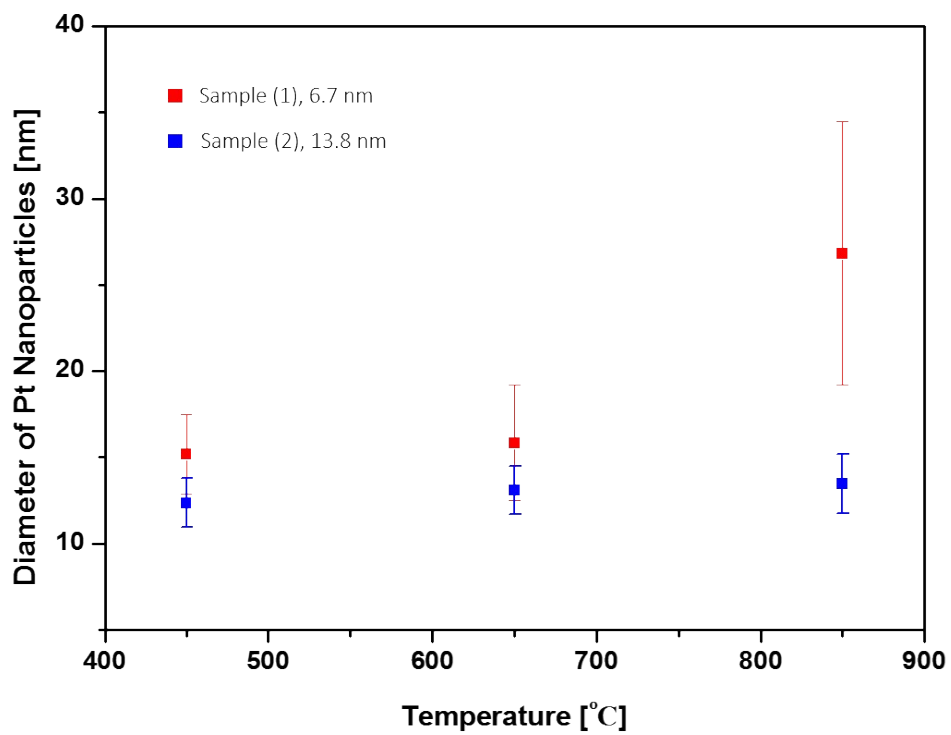


Fig. S7. The change in the size and size distribution of Pt nanoparticles in the core-shell composites after annealing at 450 °C, 650 °C, and 850 °C, respectively.

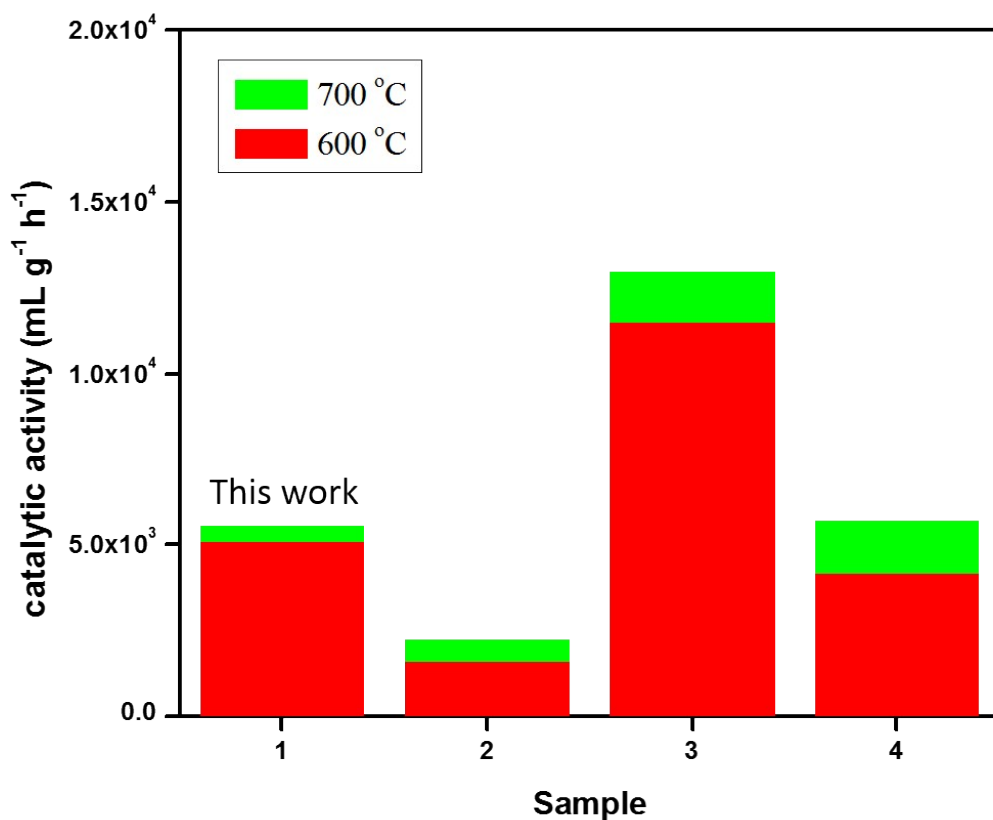


Fig. S8. Comparison of the catalytic activities for CH₄ combustion between different Pt/CeO₂ composite catalysts. #1: Pt@CeO₂ (13.8 nm) in this study, #2-4: samples reported in literatures^[1-3].

Table S2. Catalytic activity results between different Pt/CeO₂ composite catalysts.

T(°C)	Sample number	Catalytic activity (mL g ⁻¹ h ⁻¹)
600	1 (this study)	5.056E+03
	2 ^[1]	1.593E+03
	3 ^[2]	1.148E+04
	4 ^[3]	4.140E+03
700	1 (this study)	5.556E+03
	2 ^[1]	2.238E+03
	3 ^[2]	1.296E+04
	4 ^[3]	5.700E+03

References

- (1) Y. Zhu, S. Zhang, J-J Shan, L. Nguyen, S. Zhan, X. Gu, and F. Tao, *ACS Catal.*, 2013, **3**, 2627-2639.
- (2) W. Tang, Z. Hu, M. Wang, G. D. Stucky, H. Metiu, and E. W. McFarland, *J. Catal.*, 2010, **273**, 125-137.
- (3) P. Pantu, G. R. Gavalas, *Appl. Catal. A-Gen.*, 2002, **223**, 253-260.